Measurement-Induced Continuous Time Crystals

Midhun Krishna,[1,*] Parvinder Solanki,[1,†] Michal Hajdušek,[2,3,‡] and Sai Vinjanampathy[1,4,5,§]
[1]Department of Physics, Indian Institute of Technology-Bombay, Powai, Mumbai 400076, India
[2]Keio University Shonan Fujisawa Campus, 5322 Endo, Fujisawa, Kanagawa 252-0882, Japan
[3]Keio University Quantum Computing Center, 3-14-1 Hiyoshi, Kohoku, Yokohama, Kanagawa 223-8522, Japan
[4]Centre of Excellence in Quantum Information, Computation, Science and Technology, Indian Institute of Technology Bombay, Powai, Mumbai 400076, India
[5]Centre for Quantum Technologies, National University of Singapore, 3 Science Drive 2, 117543 Singapore, Singapore

(Received 6 July 2022; accepted 13 March 2023; published 14 April 2023)

Strong measurements usually restrict the dynamics of measured finite dimensional systems to the Zeno subspace, where subsequent evolution is unitary due to the suppression of dissipative terms. Here, we show qualitatively different behavior induced by the competition between strong measurements and the thermodynamic limit, inducing a time-translation symmetry breaking phase transition resulting in a continuous time crystal. We consider an undriven spin star model, where the central spin is subject to a strong continuous measurement, and qualify the dynamic behavior of the system in various parameter regimes. We show that above a critical value of measurement strength, the magnetization of the thermodynamically large ancilla spins, along with the central spin, develops limit-cycle oscillations.

DOI: 10.1103/PhysRevLett.130.150401

Introduction.—Quantum measurements are a central aspect of open quantum system dynamics with applications to quantum computing [1], sensing [2], communications [3], and cryptography [4]. Since measurements are nonunitary and act on a timescale different than Hamiltonian evolution, novel effects such as weak-value amplification [5], quantum Zeno [6], and anti-Zeno [7,8] effects are observed in finite systems. The Zeno freezing of the dynamics does not preclude dynamical behavior of the system, since a quantum system that is strongly measured can evolve unitarily in its Zeno subspace [9–12]. The situation becomes more subtle for many-body systems, where competition between measurement strength and thermodynamic limit can create novel phases. While such a competition has been studied to understand emergent steady states of quantum systems either measured or coupled to dissipative baths [13,14], it is an open question if time independent measurements *alone* can induce continuous time-translation symmetry breaking in open quantum systems in the thermodynamic limit. In this Letter, we answer this question in the affirmative by inducing a continuous time crystal entirely by measurements.

Time crystals are novel phases of matter with broken time-translation symmetry [15,16]. The earliest examples of these many-body nonequilibrium systems displayed breaking of the *discrete* time-translation symmetry in closed and open systems [17–25], and have been observed experimentally in a number of physical platforms [26–36]. It has been realized that dissipation plays a crucial role in breaking the continuous time-translation symmetry in otherwise quiescent systems, leading to "continuous time crystals" (CTCs) [37–47]. Here, the continuous symmetry is broken in the thermodynamic limit witnessed by the emergence of an oscillating steady state. These limit-cycle oscillations were recently observed in a continuously pumped dissipative atom-cavity system [48]. While discrete time crystals are induced by periodic driving, all existing models of continuous time crystals are induced by the presence of a constant external drive. In this Letter, we employ a time-translation invariant measurement scheme to induce dissipative phase transition in the thermodynamic limit.

Zeno-induced dissipative phase transitions.—Physical systems that exhibit dissipative phase transitions involve competition between coherent and dissipative terms. It is, however, not always the case that these terms scale extensively with the size of the system. A typical approach is to rescale the nonextensive terms [49–51], demanding that the dissipation rates scale inversely with the system size. Examples of this strategy can be found in both closed and open collective models [52–57], with CTCs being no exception.

Typical derivations of Markovian master equations from microscopic physics do not provide a path to this rescaling since system environment interactions are rarely tunable. In contrast to this, variation of measurement strength with the size of the system as a power law is more readily understood as a feasible control strategy [55]. This opens the attractive possibility of using measurements as a natural path to arbitrary power-law variation of the effective dissipation strength of open quantum systems. This, alongside typically controllable Hamiltonian terms, provides complete control of the dissipative phase transition.

Consider a subsystem of a thermodynamically large system being subjected to strong measurements. As detailed below, the measurements induce a Lindblad evolution on the remainder of the system [13,58–60]. The strength of the Lindblad evolution grows weaker with measurement strength. This implies that if the measurement strength scales suitably with the size of the unmeasured system, it is possible for extensive Hamiltonian terms to compete with the effective dissipation, causing qualitatively large changes in the steady state properties in the thermodynamic limit, heralding a dissipative phase transition.

Spin star model.—In order to demonstrate how measurements can induce the time-crystalline phase, we focus on a specific model given by the spin star system [61–63] shown in Fig. 1. A central spin interacting with N ancilla spins is described by the following Hamiltonian:

$$\hat{H}_T = \omega_c \hat{S}_z + \omega_a \hat{I}_z + \vec{S} \cdot \boldsymbol{J} \cdot \vec{I}, \tag{1}$$

where $\hat{I}_\alpha = \sum_k \hat{\sigma}_\alpha^k/2$ denotes the collective spin operators of the ancilla spins, $\vec{I} = (\hat{I}_x, \hat{I}_y, \hat{I}_z)^\intercal$, $\hat{S}_\alpha = \hat{\sigma}_\alpha/2$ denotes the spin operators of the central spin, and $\vec{S} = (\hat{S}_x, \hat{S}_y, \hat{S}_z)$. The natural frequencies of the central spin and collective ancilla spins are ω_c and ω_a, respectively. The interaction is characterized by the coupling matrix $\boldsymbol{J}$. The central spin is coupled to a measurement apparatus modeled as a zero temperature bath, inducing an open system evolution [64] of the spin star system given by

$$\dot{\zeta} = -i[\hat{H}_T, \zeta] + \Gamma \mathcal{D}[\hat{S}_-]\zeta. \tag{2}$$

Here, ζ is the state of the spin star system and $\mathcal{D}[\hat{O}]\zeta = \hat{O}\zeta\hat{O}^\dagger - \{\hat{O}^\dagger\hat{O}, \zeta\}/2$ is the Lindblad dissipator modeling the measurement with strength Γ. This strength is tunable for instance by changing the average number of photons in a cavity coupled to superconducting qubits [65] or by other approaches [66–70].

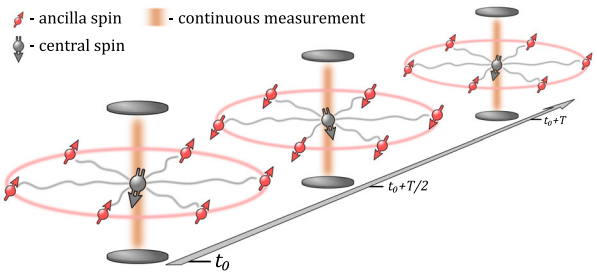

FIG. 1. Spin star model, where a single central spin interacts with multiple ancilla spins. Strong continuous measurement of the central spin induces transient oscillations of magnetization for the finite number of ancilla spins and leads to a time-translation symmetry broken phase in the thermodynamic limit. The period of these oscillations is given by $T = 2\pi/\Omega_Z$ and is explicitly calculated below.

We consider the dissipative spin star system in the Zeno limit of strong measurement and treat the Hamiltonian part perturbatively [58,59] to arrive at effective dynamics for the ancilla spins. Keeping leading order terms produces the effective master equation for ancilla spins in Lindblad form (see Supplemental Material [71]),

$$\dot{\rho} = -i[\hat{H}, \rho] + \frac{1}{\Gamma}\mathcal{D}[\hat{L}]\rho + \mathcal{O}\left(\frac{1}{\Gamma^2}\right). \tag{3}$$

Here, ρ is the reduced state of the ancilla spins, $\hat{H} = \omega_a \hat{I}_z - \frac{1}{2}\sum_\alpha J_{z\alpha}\hat{I}_\alpha$ is the effective Hamiltonian, and $\hat{L} = \sum_\alpha (J_{x\alpha}\hat{I}_\alpha - iJ_{y\alpha}\hat{I}_\alpha)$ is the jump operator for the effective dissipation. The $\mathcal{O}(1/\Gamma^2)$ correction in Eq. (3) can be neglected when $\|\hat{H}_T\|_\infty \ll \Gamma$, where $\|.\|_\infty$ is the infinity norm. We now demonstrate this by studying the Liouville eigenspectrum of the full spin star system alongside the ancilla subsystem.

Liouville eigenspectra and Zeno limit.—The Liouville eigenspectrum encodes both the transient and steady state behavior of open system dynamics [23,72–75]. Both master equations for the open spin star system in Eq. (2) and the ancilla spins in Eq. (3) can be written in the form of vectorized density matrices as $|\dot{\rho}\rangle\!\rangle = \mathcal{L}|\rho\rangle\!\rangle$ [72]. The spectral decomposition of a Liouvillian can be expressed as $\mathcal{L} = \sum_k \lambda_k |l_k\rangle\!\rangle\langle\!\langle r_k|$, where $\lambda_k = \alpha_k + i\beta_k$ are the complex eigenvalues with corresponding left and right eigenvectors $|l_k\rangle\!\rangle$ and $|r_k\rangle\!\rangle$.

The dissipator $\mathcal{D}[\hat{S}_-]$ when restricted to the central spin has four eigenstates with eigenvalues $\{0, -1/2, -1/2, -1\}$. In the full Liouville space of the spin star system, when the Hamiltonian part is not considered, these eigenvalues become $\{0, -\Gamma/2, -\Gamma/2, -\Gamma\}$, each having degeneracy given by the dimension of the ancilla Liouville space. The Hamiltonian in Eq. (2) does not commute with the dissipative term, therefore lifting the degeneracy of the full Liouvillian. Hence the Liouville eigenspectrum of the entire system shows the eigenvalues occupy vertical stripes with horizontal separation of $\mathcal{O}(\Gamma)$ between them, and a spread within each stripe of $\mathcal{O}(1/\Gamma)$, as seen in Fig. 2. Since the eigenvalues of $\mathcal{D}[\hat{S}^-]$ are purely real, the vertical spread of the spectrum depends only on the parameters of the Hamiltonian and is independent of the measurement strength Γ. We label the eigenvalues of the full Liouvillian as $\{\lambda_k^{(\mu)}\}_{\mu=\{0,1,2,3\}}$, with superscript μ denoting the vertical stripe and subscript $k < 4(N+1)^2$ enumerating the eigenvalues of the full Liouvillian within the symmetric space of the ancilla spins.

In the Zeno limit of strong measurement, the dynamics is confined in the steady state subspace of the dissipator, referred to as the Zeno subspace [9,11,12]. For Eq. (2), the Zeno subspace is given by the central spin being in the ground state, corresponding to the $\mu = 0$ stripe of the eigenspectrum. We note that the effective dynamics inside

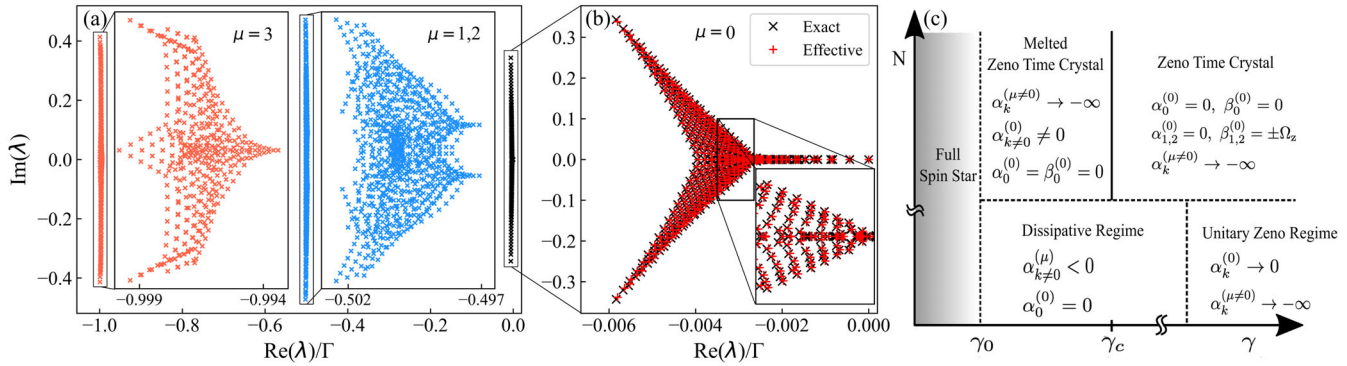

FIG. 2. Eigenspectrum of the spin star Liouvillian superoperator has four stripes ($\mu = 0, 1, 2, 3$) corresponding to different eigenvalues of Lindblad dissipator as shown in (a). Subfigure (b) shows that stripe $\mu = 0$ of the spin star Liouvillian ($\times$ in black) matches well with the effective ancilla Liouvillian ($+$ in red) for moderate reduced measurement strength of $\gamma = 15$. Corresponding nonzero Hamiltonian parameters are $\omega_c/J_{xx} = 0.1$, $\omega_a/J_{xx} = 0.01$ $J_{yy}/J_{xx} = 1$, $J_{zx}/J_{xx} = 0.01$, and $N = 20$. Competition between reduced measurement strength γ and system size N gives rise to regions of qualitatively different behavior in the parameter space as presented in (c). The dotted lines are soft boundaries with the kinks on γ and N axis representing the Zeno limit and thermodynamic limit, respectively. The effective ancilla master equation is valid in the region on right side of vertical dotted line at γ_0. The presence of phase transition is represented by the solid vertical line at critical point γ_c.

the Zeno subspace described by Eq. (3) has the Lindblad structure with weak dissipation. The difference in the eigenvalues of the full spin star Liouvillian and the ancilla Liouvillian scales as Γ^{-2}, implying nearly overlapping spectra for large enough measurement strengths [58,60]. To compare the effect of the measurement strength and the system size on the dynamics, we define the reduced measurement strength γ, such that $\Gamma = \gamma I$, with $I = N/2$ being the total spin of the ancilla subsystem.

In order to neglect the higher-order term in Eq. (3), we require the reduced measurement strength γ to be much greater than a threshold strength $\gamma_0 \approx \max\{J_{ij}, \omega_c, \omega_a\}$. For parameters chosen in Fig. 2(a), moderate value of $\gamma = 15$ shows segregation of the eigenspectrum of spin star Liouvillian into distinct stripes. Figure 2(b) shows excellent agreement between the Liouville eigenspectrum of the full and effective evolutions given by Eq. (2) and Eq. (3), respectively.

The Zeno limit of $\Gamma \to \infty$ can be achieved either by keeping the system size fixed and increasing the reduced measurement strength ($\gamma \to \infty$) or by keeping the reduced measurement strength constant and going to the thermodynamic limit ($N \to \infty$). Depending on the value of γ and N, the spin star model shows distinct dynamical behavior as sketched in Fig. 2(c). We explore these further below, assuming that $\gamma \gg \gamma_0$.

Finite spin star system.—As the strength of measurement on the central spin increases, the effective dissipation on the collective ancilla spin becomes weaker. For a finite ancilla size depending on the value of γ, we observe two distinct regimes. These regimes are referred to as "dissipative regime" and "unitary Zeno regime" in Fig. 2(c). In the dissipative regime, all the eigenvalues of the spin star Liouvillian, except the one corresponding to a steady state, have finite real part, $\alpha^{\mu}_{k\neq 0} < 0$. Hence the dynamics takes arbitrary initial symmetric states of the ancilla spins to the steady state characterized by $\lambda_0 = 0$. In contrast, in the unitary Zeno regime when $\gamma \to \infty$, the dissipation inside the Zeno subspace vanishes and the dynamics of collective ancilla spins is unitary [9,10]. In terms of the Liouville eigenspectrum of the spin star system, the unitary Zeno regime can be viewed as the collapse of the steady state stripe onto the imaginary axis, $\alpha^0_k \to 1/\Gamma \to 0$, and the divergence of the eigenvalues from the other stripes toward negative infinity $\alpha^{\mu\neq 0}_k \to -\Gamma \to -\infty$. In this limit, the measurement overwhelms the dynamics of the central spin and drives it to a steady state given by $\langle \vec{S} \rangle = (0, 0, -1/2)$, essentially decoupling it from the ancilla spins. We now show that variation of measurement strength induces strikingly different behavior in the thermodynamic limit.

Thermodynamic limit.—In contrast to the previous section, we choose a fixed value of the reduced measurement strength $\gamma \gg \gamma_0$ and let the number of the ancilla spins diverge, $N \to \infty$. Doing this opens the possibility for a dissipative phase transition to occur, as both the unitary and dissipative parts of the master equation, Eq. (3), scale extensively with the size of the system. To illustrate this, we make a particular choice for the coupling matrix $\boldsymbol{J}$ with nonzero entries $J_{xx} = J_{yy}, J_{zz} = 2\omega_a$ and $J_{zx} = -2\Omega$. Such anisotropic terms can be engineered by directional hopping in Fermionic models [76–78] or optical lattices. This choice of parameters reduces the ancilla master equation to

$$\dot{\rho} = -i\Omega[\hat{I}_x, \rho] + \frac{\kappa}{I}\mathcal{D}[\hat{I}_-]\rho, \tag{4}$$

where $\kappa := J^2_{xx}/\gamma$ is the effective dissipation rate. This is the well-known driven Dicke model of continuous time

crystallization [37,43–45]. Equation (4) displays a dissipative phase transition between a stationary melted phase for $\Omega/\kappa \leq 1$ and a CTC phase for $\Omega/\kappa > 1$ [37], where the system self-organizes into a steady state with persistent limit-cycle oscillations. An alternate form of CTC with Lindblad dissipator of the form $\mathcal{D}[\hat{S}_+]$ can be engineered by coupling central spin to inverted bath or by choosing a different choice for coupling matrix (see Supplemental Material [71]).

We note that the phase transition occurs at the critical reduced measurement strength $\gamma_c = J_{xx}^2/\Omega$. This implies that for reduced measurement strength $\gamma_0 \ll \gamma \leq \gamma_c$, the ancilla spins are in a stationary phase, where the effective dissipation dominates over the coherent evolution. In contrast, when $\gamma > \gamma_c \gg \gamma_0$, the ancilla spins enter a CTC phase with persistent oscillations of their magnetization, breaking the time-translation symmetry of the underlying dynamics, as seen in Fig. 2(c).

The emergence of limit cycles in CTCs is traditionally understood as a competition between oscillations-inducing coherent drive and oscillations-destroying dissipation [37,39,43,79–82]. We note the absence of any coherent drive in the full spin star model of Eq. (2). The key ingredients in our model are anisotropic coupling of the central spin to the ancilla spins given by finite off-diagonal element of the coupling matrix $\boldsymbol{J}$ and the Zeno limit given by diverging measurement strength Γ. In order to distinguish the origin of the effective model in Eq. (4) from more traditional models in literature, we refer to this measurement-induced symmetry-broken phase as a "Zeno time crystal" (ZTC).

The ZTC phase can be witnessed by examining the Liouville eigenspectrum of the full spin star model in Eq. (2). In the Zeno limit taken by $N \to \infty$ for a fixed reduced measurement strength γ, the asymptotic dynamics settles into oscillating coherences. These are eigenstates of Eq. (2) located within $\mu = 0$ stripe with pure imaginary eigenvalues $\lambda_{1,2} = \pm i\Omega_Z$, where $\Omega_Z = \sqrt{(J_{xx}^2/\gamma)^2 - \Omega^2}$ is the frequency of the limit-cycle oscillations. Eigenstates with eigenvalues located within the remaining stripes, $\mu \neq 0$, have eigenvalues with nonvanishing real parts and therefore have no effect on late-time dynamics.

We plot the dynamics of the rescaled magnetization of the ancilla spins, $m_z \equiv \langle \hat{I}_z \rangle / N$, in Fig. 3(a) for increasing values of N. We observe that for rescaled measurement strength $\gamma \leq \gamma_c$, m_z settles into a steady value. This is represented by the dashed lines and corresponds to the melted ZTC phase of Fig. 2(c). On the other hand, for $\gamma > \gamma_c$, the rescaled magnetization of the ancilla spins displays transient oscillations for finite N as represented by the solid lines in Fig. 3(a). The stability of these oscillations increases with the number of ancilla spins N. In the thermodynamic limit, $N \to \infty$, these oscillations become persistent, signaling a genuine phase with broken time-translation symmetry. The full system of nonlinear mean-field equations for $\langle \hat{I}_\alpha \rangle$ as well as the central spin $\langle \hat{S}_\alpha \rangle$ can be found in [71].

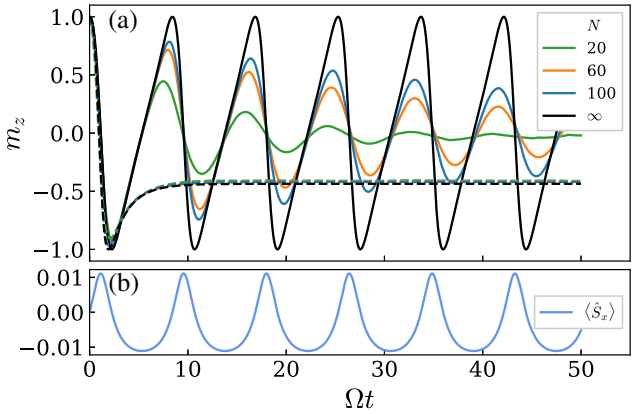

FIG. 3. (a) Time evolution of rescaled ancilla spin operator m_z for varying numbers of ancilla spins for initial state $\vec{m} = (0, 0, 1)$. The solid lines correspond to the dynamics in the ZTC phase with $\Omega/\kappa = 1.5$, and show longer-lived oscillations as N increases. These oscillations become persistent in the thermodynamic limit. The dashed lines correspond to the melted phase with $\Omega/\kappa = 0.9$, for which m_z settles down to a saddle fixed point. (b) Magnetization $\langle \hat{S}_x \rangle$ of the central spin oscillates with the same frequency as the ancilla spins.

For completeness, we examine the dynamics of the central spin in the Zeno limit and diverging number of ancilla spins N. The evolution of the central spin is dominated by the measurement strength Γ, resulting in rapid damping of $\langle \vec{S} \rangle$. Solving the mean-field dynamics of the coupled system in the Zeno limit using adiabatic elimination [83] leads to the steady state solution for the central spin given by $\langle \vec{S} \rangle \approx (-J_{xx} m_y/\gamma, J_{xx} m_x/\gamma, -1/2)$. Since the rescaled magnetization of the ancilla spins, m_x and m_y, display limit-cycle oscillations in the ZTC phase, so does the magnetization of the central spin, as shown in Fig. 3(b) where we plot the steady state dynamics of $\langle \hat{S}_x \rangle$. This demonstrates that time-translation symmetry breaking does not only occur in the ancilla spins but in the central spin as well. We see that provided $\gamma > \gamma_c$, the central spin oscillates with the same frequency as the ancilla spins.

Conclusions.—In this Letter, we provide a path to observe continuous time-translation symmetry breaking in many-body phase transitions induced by static quantum measurements alone. We demonstrate how to observe Zeno time crystals in spin star system where the entire system, including the central spin, oscillates in time. The spin star system is well studied both theoretically [62,63,84–87] and experimentally [88–91], forming a suitable platform for stable quantum technologies. The relationship between phase coherence, limit cycles, and quantum technologies has been studied recently in a number of physical systems [75,92–95]. Our result is intriguing in the role quantum measurements have played in phase transitions. Unlike

previous models, which involve explicit coherent drive, we can observe time crystallinity directly from the strong measurement of a subsystem, which provides both the coherent and dissipative terms for the time crystal. Furthermore, these local measurements are usually thought of as localizing the wave function and hence disrupting the otherwise entangling nature of the unitary evolution in the study of measurement-induced phase transitions [96–98]. The results presented here are contrary to that expectation as well, since indeed only in the strong measurement limit do we see effective correlations being built up in the ancilla spins causing time-crystalline behavior.

We note that our methods have elaborated how environment engineering of the ancilla spins in a spin star model can be achieved by careful selection of the coupling Hamiltonian and measurement rates. Our results present a novel technique of controlling the spin star model. While inhomogeneous interactions have been shown to produce complete controllability of the ancilla spins [99], here we demonstrate that sufficient coherent control of the ancilla spins is available even in the thermodynamic limit with anisotropic interactions. Such bath engineering can be used to devise technology applications such as quantum memories, which rely on coherences [72]. For a finitely large number of spins and for finitely strong measurements, we can expect a metastable CTC whose spectral gap goes as $1/\Gamma$. We hence expect this Letter to benefit our foundational understanding of phase transitions and provide a concrete pathway to realistic quantum technology applications.

M. K. acknowledges support by Prime Minister's Research Fellows (PMRF) scheme offered by the Ministry of Education, Government of India. M. H. is supported by MEXT Quantum Leap Flagship Program Grants No. JPMXS0118067285 and No. JPMXS01 20319794. S. V. acknowledges support from a DST-SERB Early Career Research Award (ECR/2018/000957) and DST-QUEST grant no. DST/ICPS/QuST/Theme-4/2019. S. V. thanks L. Garbe, S. R. Hassan, V. R. Krithika, T. S. Mahesh, V. Mukherjee, B. Prasanna Venkatesh, and J. Thingna for useful discussions.

*Corresponding author.
midhunkrishna@iitb.ac.in
†Corresponding author.
psolanki@phy.iitb.ac.in
‡Corresponding author.
michal@sfc.wide.ad.jp
§Corresponding author.
sai@phy.iitb.ac.in

[1] R. Raussendorf and H. J. Briegel, Phys. Rev. Lett. **86**, 5188 (2001).
[2] C. L. Degen, F. Reinhard, and P. Cappellaro, Rev. Mod. Phys. **89**, 035002 (2017).
[3] S. Khatri and M. M. Wilde, arXiv:2011.04672.
[4] N. Gisin, G. Ribordy, W. Tittel, and H. Zbinden, Rev. Mod. Phys. **74**, 145 (2002).
[5] Y. Aharonov, D. Z. Albert, and L. Vaidman, Phys. Rev. Lett. **60**, 1351 (1988).
[6] B. Misra and E. C. G. Sudarshan, J. Math. Phys. (N.Y.) **18**, 756 (1977).
[7] B. Kaulakys and V. Gontis, Phys. Rev. A **56**, 1131 (1997).
[8] V. Mukherjee, A. G. Kofman, and G. Kurizki, Commun. Phys. **3**, 1 (2020).
[9] D. Burgarth, P. Facchi, H. Nakazato, S. Pascazio, and K. Yuasa, Quantum **3**, 152 (2019).
[10] P. Zanardi and L. Campos Venuti, Phys. Rev. Lett. **113**, 240406 (2014).
[11] P. Facchi and S. Pascazio, Phys. Rev. Lett. **89**, 080401 (2002).
[12] P. Facchi and S. Pascazio, J. Phys. A **41**, 493001 (2008).
[13] E. M. Kessler, G. Giedke, A. Imamoglu, S. F. Yelin, M. D. Lukin, and J. I. Cirac, Phys. Rev. A **86**, 012116 (2012).
[14] M. Seclì, M. Capone, and M. Schirò, Phys. Rev. A **106**, 013707 (2022).
[15] K. Sacha and J. Zakrzewski, Rep. Prog. Phys. **81**, 016401 (2017).
[16] D. V. Else, C. Monroe, C. Nayak, and N. Y. Yao, Annu. Rev. Condens. Matter Phys. **11**, 467 (2020).
[17] D. V. Else, B. Bauer, and C. Nayak, Phys. Rev. Lett. **117**, 090402 (2016).
[18] A. Russomanno, F. Iemini, M. Dalmonte, and R. Fazio, Phys. Rev. B **95**, 214307 (2017).
[19] F. M. Surace, A. Russomanno, M. Dalmonte, A. Silva, R. Fazio, and F. Iemini, Phys. Rev. B **99**, 104303 (2019).
[20] R. Khasseh, R. Fazio, S. Ruffo, and A. Russomanno, Phys. Rev. Lett. **123**, 184301 (2019).
[21] Z. Gong, R. Hamazaki, and M. Ueda, Phys. Rev. Lett. **120**, 040404 (2018).
[22] A. Lazarides, S. Roy, F. Piazza, and R. Moessner, Phys. Rev. Res. **2**, 022002(R) (2020).
[23] A. Riera-Campeny, M. Moreno-Cardoner, and A. Sanpera, Quantum **4**, 270 (2020).
[24] A. Cabot, F. Carollo, and I. Lesanovsky, Phys. Rev. B **106**, 134311 (2022).
[25] R. J. L. Tuquero, J. Skulte, L. Mathey, and J. G. Cosme, Phys. Rev. A **105**, 043311 (2022).
[26] J. Zhang, P. W. Hess, A. Kyprianidis, P. Becker, A. Lee, J. Smith, G. Pagano, I. D. Potirniche, A. C. Potter, A. Vishwanath, N. Y. Yao, and C. Monroe, Nature (London) **543**, 217 (2017).
[27] S. Choi, J. Choi, R. Landig, G. Kucsko, H. Zhou, J. Isoya, F. Jelezko, S. Onoda, H. Sumiya, V. Khemani, C. von Keyserlingk, N. Y. Yao, E. Demler, and M. D. Lukin, Nature (London) **543**, 221 (2017).
[28] S. Pal, N. Nishad, T. S. Mahesh, and G. J. Sreejith, Phys. Rev. Lett. **120**, 180602 (2018).
[29] J. Rovny, R. L. Blum, and S. E. Barrett, Phys. Rev. Lett. **120**, 180603 (2018).
[30] J. Smits, L. Liao, H. T. C. Stoof, and P. van der Straten, Phys. Rev. Lett. **121**, 185301 (2018).
[31] A. Kyprianidis, F. Machado, W. Morong, P. Becker, K. S. Collins, D. V. Else, L. Feng, P. W. Hess, C. Nayak, G. Pagano, N. Y. Yao, and C. Monroe, Science **372**, 1192 (2021).

[32] H. Taheri, A. B. Matsko, L. Maleki, and K. Sacha, Nat. Commun. **13**, 848 (2022).
[33] H. Keßler, P. Kongkhambut, C. Georges, L. Mathey, J. G. Cosme, and A. Hemmerich, Phys. Rev. Lett. **127**, 043602 (2021).
[34] X. Mi, M. Ippoliti, C. Quintana, A. Greene, Z. Chen, J. Gross, F. Arute, K. Arya, J. Atalaya, R. Babbush *et al.*, Nature (London) **601**, 531 (2022).
[35] P. Frey and S. Rachel, Sci. Adv. **8**, eabm7652 (2021).
[36] J. Randall, C. E. Bradley, F. V. van der Gronden, A. Galicia, M. H. Abobeih, M. Markham, D. J. Twitchen, F. Machado, N. Y. Yao, and T. H. Taminiau, Science **374**, 1474 (2021).
[37] F. Iemini, A. Russomanno, J. Keeling, M. Schirò, M. Dalmonte, and R. Fazio, Phys. Rev. Lett. **121**, 035301 (2018).
[38] K. Tucker, B. Zhu, R. J. Lewis-Swan, J. Marino, F. Jimenez, J. G. Restrepo, and A. M. Rey, New J. Phys. **20**, 123003 (2018).
[39] B. Buča, J. Tindall, and D. Jaksch, Nat. Commun. **10**, 1730 (2019).
[40] B. Zhu, J. Marino, N. Y. Yao, M. D. Lukin, and E. A. Demler, New J. Phys. **21**, 073028 (2019).
[41] C. Lledó, T. K. Mavrogordatos, and M. H. Szymańska, Phys. Rev. B **100**, 054303 (2019).
[42] K. Seibold, R. Rota, and V. Savona, Phys. Rev. A **101**, 033839 (2020).
[43] L. F. d. Prazeres, L. d. S. Souza, and F. Iemini, Phys. Rev. B **103**, 184308 (2021).
[44] G. Piccitto, M. Wauters, F. Nori, and N. Shammah, Phys. Rev. B **104**, 014307 (2021).
[45] F. Carollo and I. Lesanovsky, Phys. Rev. A **105**, L040202 (2022).
[46] M. Hajdušek, P. Solanki, R. Fazio, and S. Vinjanampathy, Phys. Rev. Lett. **128**, 080603 (2022).
[47] Y. Nakanishi and T. Sasamoto, Phys. Rev. A **107**, L010201 (2023).
[48] P. Kongkhambut, J. Skulte, L. Mathey, J. G. Cosme, A. Hemmerich, and H. Keßler, Science **377**, 6606 (2022).
[49] N. Defenu, T. Donner, T. Macrì, G. Pagano, S. Ruffo, and A. Trombettoni, arXiv:2109.01063.
[50] C. Anteneodo and C. Tsallis, Phys. Rev. Lett. **80**, 5313 (1998).
[51] P. Kirton, M. M. Roses, J. Keeling, and E. G. Dalla Torre, Adv. Quantum Technol. **2**, 1800043 (2019).
[52] V. M. Bastidas, C. Emary, B. Regler, and T. Brandes, Phys. Rev. Lett. **108**, 043003 (2012).
[53] J. S. Ferreira and P. Ribeiro, Phys. Rev. B **100**, 184422 (2019).
[54] M.-J. Hwang and M. B. Plenio, Phys. Rev. Lett. **117**, 123602 (2016).
[55] L. Garbe, I. Egusquiza, E. Solano, C. Ciuti, T. Coudreau, P. Milman, and S. Felicetti, Phys. Rev. A **95**, 053854 (2017).
[56] L. Bakker, M. Bahovadinov, D. Kurlov, V. Gritsev, A. K. Fedorov, and D. Krimer, Phys. Rev. Lett. **129**, 250401 (2022).
[57] F. Minganti, A. Biella, N. Bartolo, and C. Ciuti, Phys. Rev. A **98**, 042118 (2018).
[58] V. Popkov, S. Essink, C. Presilla, and G. Schütz, Phys. Rev. A **98**, 052110 (2018).
[59] E. M. Kessler, Phys. Rev. A **86**, 012126 (2012).
[60] V. Popkov and C. Presilla, Phys. Rev. Lett. **126**, 190402 (2021).
[61] A. Hutton and S. Bose, Phys. Rev. A **69**, 042312 (2004).
[62] E. Barnes, Ł. Cywiński, and S. D. Sarma, Phys. Rev. Lett. **109**, 140403 (2012).
[63] M. Bortz and J. Stolze, Phys. Rev. B **76**, 014304 (2007).
[64] H.-P. Breuer, F. Petruccione *et al.*, *The Theory of Open Quantum Systems* (Oxford University Press on Demand, New York, 2002).
[65] P. M. Harrington, J. T. Monroe, and K. W. Murch, Phys. Rev. Lett. **118**, 240401 (2017).
[66] K. Jacobs and D. A. Steck, Contemp. Phys. **47**, 279 (2006).
[67] J. Javanainen and J. Ruostekoski, New J. Phys. **15**, 013005 (2013).
[68] D. H. Slichter, R. Vijay, S. J. Weber, S. Boutin, M. Boissonneault, J. M. Gambetta, A. Blais, and I. Siddiqi, Phys. Rev. Lett. **109**, 153601 (2012).
[69] C. Simonelli, M. Archimi, L. Asteria, D. Capecchi, G. Masella, E. Arimondo, D. Ciampini, and O. Morsch, Phys. Rev. A **96**, 043411 (2017).
[70] F. Schäfer, I. Herrera, S. Cherukattil, C. Lovecchio, F. S. Cataliotti, F. Caruso, and A. Smerzi, Nat. Commun. **5**, 3194 (2014).
[71] See Supplemental Material at http://link.aps.org/supplemental/10.1103/PhysRevLett.130.150401 for derivation of effective master equation and mean-field analysis.
[72] V. V. Albert and L. Jiang, Phys. Rev. A **89**, 022118 (2014).
[73] K. Macieszczak, M. Guţă, I. Lesanovsky, and J. P. Garrahan, Phys. Rev. Lett. **116**, 240404 (2016).
[74] P. Solanki, N. Jaseem, M. Hajdušek, and S. Vinjanampathy, Phys. Rev. A **105**, L020401 (2022).
[75] N. Jaseem, M. Hajdušek, P. Solanki, L.-C. Kwek, R. Fazio, and S. Vinjanampathy, Phys. Rev. Res. **2**, 043287 (2020).
[76] E. J. Bergholtz, J. C. Budich, and F. K. Kunst, Rev. Mod. Phys. **93**, 015005 (2021).
[77] S. R. Hassan, P. V. Sriluckshmy, S. K. Goyal, R. Shankar, and D. Sénéchal, Phys. Rev. Lett. **110**, 037201 (2013).
[78] V. Borisov, Y. O. Kvashnin, N. Ntallis, D. Thonig, P. Thunström, M. Pereiro, A. Bergman, E. Sjöqvist, A. Delin, L. Nordström, and O. Eriksson, Phys. Rev. B **103**, 174422 (2021).
[79] H. Keßler, J. G. Cosme, M. Hemmerling, L. Mathey, and A. Hemmerich, Phys. Rev. A **99**, 053605 (2019).
[80] B. Buča and D. Jaksch, Phys. Rev. Lett. **123**, 260401 (2019).
[81] D. Nishant, L. Manuele, K. Katrin, H. Lorenz, D. Tobias, and E. Tilman, Science **366**, 1496 (2019).
[82] Z. Zhang, D. Dreon, T. Esslinger, D. Jaksch, B. Buca, and T. Donner, arXiv:2205.01461.
[83] H. Haken, *Synergetics. An Introduction. Nonequilibrium Phase Trasitions and Self-organization in Physics, Chemistry, and Biology* (Springer, New York, 1977).
[84] J. Fischer, B. Trauzettel, and D. Loss, Phys. Rev. B **80**, 155401 (2009).
[85] A. Faribault and D. Schuricht, Phys. Rev. Lett. **110**, 040405 (2013).
[86] R. van den Berg, G. Brandino, O. El Araby, R. Konik, V. Gritsev, and J.-S. Caux, Phys. Rev. B **90**, 155117 (2014).

[87] U. Seifert, P. Bleicker, P. Schering, A. Faribault, and G. S. Uhrig, Phys. Rev. B **94**, 094308 (2016).
[88] T. Mahesh, D. Khurana, V. Krithika, G. Sreejith, and C. S. Kumar, J. Phys. Condens. Matter **33**, 383002 (2021).
[89] D. Suter and F. Jelezko, Prog. Nucl. Magn. Reson. Spectrosc. **98**, 50 (2017).
[90] C. E. Bradley, J. Randall, M. H. Abobeih, R. Berrevoets, M. Degen, M. A. Bakker, M. Markham, D. Twitchen, and T. H. Taminiau, Phys. Rev. X **9**, 031045 (2019).
[91] F. Poggiali, P. Cappellaro, and N. Fabbri, Phys. Rev. B **95**, 195308 (2017).
[92] S. Sonar, M. Hajdušek, M. Mukherjee, R. Fazio, V. Vedral, S. Vinjanampathy, and L.-C. Kwek, Phys. Rev. Lett. **120**, 163601 (2018).
[93] N. Jaseem, M. Hajdušek, V. Vedral, R. Fazio, L.-C. Kwek, and S. Vinjanampathy, Phys. Rev. E **101**, 020201(R) (2020).
[94] A. W. Laskar, P. Adhikary, S. Mondal, P. Katiyar, S. Vinjanampathy, and S. Ghosh, Phys. Rev. Lett. **125**, 013601 (2020).
[95] V. R. Krithika, P. Solanki, S. Vinjanampathy, and T. S. Mahesh, Phys. Rev. A **105**, 062206 (2022).
[96] D. Rossini and E. Vicari, Phys. Rep. **936**, 1 (2021).
[97] J. M. Koh, S.-N. Sun, M. Motta, and A. J. Minnich, arXiv:2203.04338.
[98] B. Skinner, J. Ruhman, and A. Nahum, Phys. Rev. X **9**, 031009 (2019).
[99] C. Arenz, G. Gualdi, and D. Burgarth, New J. Phys. **16**, 065023 (2014).